Power optimization for phase quantization with SOAs using the gain extinction ratio

ANEESH SOBHANAN,[1] **ARJUN IYER,**[1,2] **ARAVIND ANTHUR,**[3,4]
GOVIND P. AGRAWAL,[5] **LIAM P. BARRY,**[3]
AND DEEPA VENKITESH[1,*]

[1]*Department of Electrical Engineering, Indian Institute of Technology Madras, Chennai 600 036, India*
[2]*Currently at University of Rochester, Rochester, New York 14627, USA*
[3]*School of Electronic Engineering, Dublin City University, Dublin, Ireland*
[4]*Currently at Agency for Science, Technology and Research, Singapore*
[5]*The Institute of Optics, University of Rochester, Rochester, New York 14627, USA*
[*]deepa@ee.iitm.ac.in

Abstract: Phase-sensitive amplifiers (PSAs) can work as $M-$ level phase quantizers when waves generated with specific phase values are allowed to mix coherently in a nonlinear medium. The quality of an $M-$ level phase quantizer depends on the relative powers of the mixing waves and requires their optimization. If the mixing waves also experience gain in the nonlinear medium, such as in semiconductor optical amplifiers (SOAs), this optimization becomes non-trivial. In this paper, we present a general method to optimize phase quantization using a PSA made using an SOA, based on gain extinction ratio (*GER*), which is an experimentally measurable quantity. We present a simple theory to derive the optimal *GER* required to achieve an $M-$level quantization. We further experimentally demonstrate two- and four-level phase quantization schemes with an SOA, operated at the optimized *GER*, with pump power levels as low as 1 mW.

1. Introduction

Amplitude regeneration of intensity modulated data using all-optical signal processing has been reported widely in the past [1–3]. The advent of coherent optical communication demands the attention of such optical processing towards phase regeneration. The squeezing function of phase sensitive amplifiers (PSAs) enables phase regeneration, where the signal and noise are amplified in the quadrature that carries information while they are attenuated in the conjugate quadrature [4,5]. In addition to optical communication, PSAs have a wide range of applications including for large scale Ising spin networks [6], phase measurement with enhanced sensitivity [7] and quantum metrology [8]. Four-wave mixing inside a highly nonlinear fiber (HNLF) is usually employed for realizing PSA [9]. A key performance indicator of any PSA is the gain extinction ratio (*GER*), defined as the ratio of maximum to minimum phase-sensitive gain. There have been many PSA demonstrations in the past, with GERs as large as 30 dB [10–13]. One of the earlier numerical studies on PSA for QPSK phase regeneration was carried out using a Sagnac interferometer configuration [14]. Since then, there have been several reports, including black-box implementations of a PSA with a pump phase-locking stage for BPSK and QPSK modulation, with an HNLF as the nonlinear medium [15–19]. Multi-channel phase regeneration using a polarization-assisted PSA was demonstrated in [20]. The use of multi-wave interference to improve the phase-quantization was shown in [21]. Polarization-diversity schemes for PSA were investigated further using HNLF in [22–26] for polarization-insensitive phase regeneration of polarization-multiplexed phase-modulated data.

Practical implementations of the fiber-based schemes are limited by the high pump power requirements and their relatively large footprint. A smaller footprint for PSA was reported with the use of waveguide-based nonlinear media such as periodically poled lithium niobate [27–29],

silicon germanium [30,31] and AlGaAs [32]. However, the pump power required for achieving PSA in all these media are also relatively high. Table 1 compares the pump power used in the previous reports for the demonstration of PSA-based phase regeneration and phase quantization in different nonlinear media. The two challenges, a large footprint and a large pump power, can be overcome by using SOAs, which require much smaller powers (<10 mW) to initiate nonlinear interactions and can be potentially integrated on photonic integrated circuits. There have been a few reports on realising PSA with SOAs. A monolithically integrated phase-sensitive amplification chip with SOAs was discussed in [33], where *GER* of ~7.8 dB was achieved. Regeneration of a multi-channel DPSK signal using PSA in SOAs was demonstrated in [34]. Further, all-optical phase regeneration of a QPSK signal through PSA in SOAs, was presented for the first time in [35]. However, it is commonly realized that the amplified spontaneous emission would lead to poorer noise performance when SOAs are used. This has been proved to be unfounded, and we have reported that, due to pump saturation, the OSNR of the signal and conjugate waves is maintained when SOAs are used for FWM, for an input OSNR values of <28 dB [36]. The presence of saturating pump is also found to minimize the nonlinear phase noise introduced by the SOAs [37].

Table 1. Record of PSA-based phase regeneration and phase quantization experiments in different nonlinear media with the corresponding pump power levels used.

Process	Nonlinear medium	Pump power (dBm)	Reference
Phase quantization	HNLF	27	J. Kakande et.al., [17]
		29	C. Lundström et.al., [38]
		>20	F. Parmigiani et.al., [44]
		26	A.Almaiman et.al., [45]
Phase regeneration	HNLF	33	R. Slavík et.al., [15]
		>30	R. Slavík et.al., [16]
		29	J. Yang et. al., [23].
		30	S. L. I. Olsson et.al., [51]
	PPLN	30	B. J. Puttnam et. al., [27].
		24.7	T. Umeki et. al., [28]
		21	S. Liu et.al., [50]
	SiGe Waveguide	<21	M. A. Ettabib et. al., [30,31]
	SOA	< 6	A. D. Ellis et.al., [34]
		< 7	S. Sygletos et.al., [46]
		<10	K. R. H. Bottrill et.al., [35]
Phase sensitive amplifier	PPLN	33	K. J. Lee et.al., [49]
	a-Si:H waveguide	32 (Peak power-pulsed)	H. Sun et. al., [47]
	Si-Photonic crystal waveguide	31.7 (Peak power-pulsed)	Y. Zhang, et. al., [48]
	A1GaAsOI	19 to 27	F. Da Ros et.al., [32]
Phase quantization	**SOA**	**0**	**(This work)**

One of the critical design parameters for a PSA is the *GER*, which is in turn decided by the correct choice of mixing ratios of the signal with the desired idler. Several reports in the past have described the details of optimization of power levels of the mixing beams in HNLF-based PSA [38]. The dependence of PSA gain on the phase-to-amplitude and phase-to-phase transfer functions of a PSA made using HNLF are discussed [39,40]. The dependence of the noise figure (NF) of a PSA on the different signal-idler power ratios was addressed in [41], where an experimental study was conducted with random gain values and it was concluded that the

best phase quantization is achieved when the power ratio between the signal and the conjugate are equal in case of two-level quantization. A detailed analytical formulation was presented in [42], where the optimal amplitude ratio between the signal and its harmonic was discussed for a general $M-$ level optical phase quantization of a signal with uniform phase distribution. A brute-force optimization of the quantization may be possible by adjusting the power levels at the input of the PSA when the nonlinear medium is passive. However, this may be difficult for an active gain medium such as SOA. None of the previous demonstrations of PSAs made with SOAs discuss the systematic optimization of the ratio between input signal and pump power required for optimal performance. SOAs being amplifiers provide asymmetric gain, it would be cumbersome to carry out an optimization by just randomly adjusting the power ratio of the input waves.

In this paper, we derive a relation between the signal-to-idler amplitude mixing ratio (r) and the *GER*, which is a measurable quantity at the output of the SOA, that can be used to achieve optimal $M-$level phase quantization in general. This relation is universal, and can be applied irrespective of the nonlinear medium used for the PSA. We have previously presented numerical results on the influence of *GER* on $M-$level quantization with SOA [43]. Here, we present experimental data that verifies the dependence of *GER* on the quality of phase quantization in SOA. We also quantify the phase-sensitive gain (PSG) for two and four-level phase quantization schemes, the dependence of the quality of quantization on *GER* and then discuss two and four-level phase quantization with optimized *GER*. With careful power optimization, we experimentally achieve phase quantization with a pump power of only 0 dBm. A comparison with previous work (Table 1) shows that the SOA based demonstration in this work uses the lowest pump power.

2. Theory

Phase quantization is implemented typically through a non-degenerate FWM process occurring inside a nonlinear medium. The schematic of a FWM- based M-level phase quantizer is shown in Fig. 1(a) [17]. Two pumps with frequencies f_{p1} and f_{p2} and powers P_{p1} and P_{p2} respectively are allowed to mix with the signal at frequency f_s, with power P_s, whose phase ϕ_s is to be quantized to M levels. Assuming δf to be the frequency separation between the pump1 and the signal, the pump frequencies are chosen such that $f_{p2} - f_{p1} = M\delta f$ and $f_{p2} - f_s = (M - 1)\delta f$ as shown in Fig. 1(a). These two pumps and signal should be phase correlated for realizing phase quantization.
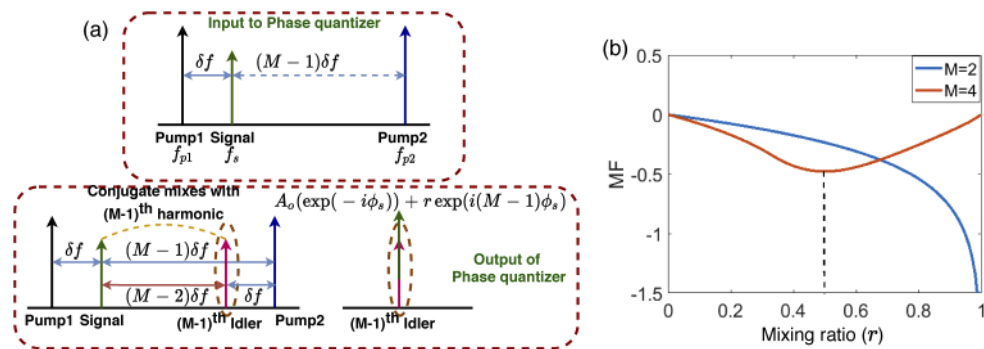

Fig. 1. (a) Schematic of the input and output spectral components of an $M-$ level phase quantizer, the output spectrum indicates the mixing frequencies that result in an M-level quantization. (b) Misfit factor as a function of the mixing ratio, r for $M = 2, 4$

Cascaded FWM of the pump 1 and the signal generates the $(M - 1)^{th}$ idler at frequency $f_{p2} - \delta f$, with a phase $(M - 1)\phi_s$. This idler is allowed to coherently mix with the conjugate idler generated by the non-degenerate mixing of pump 1, pump 2 and the signal at the frequency

$f_{p1} + f_{p2} - f_s = f_{p2} - \delta f$ and phase, $-\phi_s$. The complex amplitude A_{out} of this coherent combination can be written as,

$$A_{out} = A_0 \exp(-i\phi_s) + rA_0 \exp\left(i(M-1)\phi_s\right), \tag{1}$$

where A_0, rA_0, are the amplitudes of the two mixing fields at the idler frequency. The quality of this interference output and hence that of the quantization depends on the mixing ratio r, which is decided by the conversion efficiency of the mixing process. The importance of the choice of r for an $M-$ level quantization is studied in detail in [17], where the average deviation of the proposed phase quantizer from an ideal step function is quantified through a misfit factor (*MF*), defined as,

$$MF = \log_{10}\left(\frac{M^2}{\pi^2} \int_{-\frac{\pi}{M}}^{\frac{\pi}{M}} |\phi_o(r, \phi_s) - \phi_{step}| d\phi_s\right), \tag{2}$$

where ϕ_s is the input phase to be quantized, ϕ_o is the phase of the output field defined in Eq. (1), and ϕ_{step} is the ideal step function. Figure 1(b) shows the *MF* as a function of r for $M = 2$ and 4. The *MF* of an ideally quantized output would tend to $-\infty$. For the two-level phase quantization, the value of r that leads to the ideal *MF* is 1, as seen in Fig. 1(b), indicating that optimal quantization occurs when the conjugate and the requisite idler mixes with equal amplitudes. This conclusion has been previously verified through experiments using HNLF in [39]. The optimal mixing ratio progressively decreases with increasing M. For $M = 4$, *MF* is found to be minimum at $r = 0.5$. Since r is not measurable directly in an experiment, especially when the nonlinear medium is a gain medium as in our case, we propose to quantify r through the *GER*, defined as the ratio of the maximum output gain to the minimum output gain when ϕ_s is tuned over 2π. For a process governed by Eq. (1), the output power P_{out} is given by

$$P_{out} = |A_{out}|^2 = A_o^2(1 + r^2 + 2r\cos(M\phi_s)). \tag{3}$$

GER can be a analytically derived from the output power as,

$$GER = 10\log_{10}\left(\frac{P_{out,max}}{P_{out,min}}\right) = 10\log_{10}\left(\frac{1+r}{1-r}\right)^2 \tag{4}$$

Thus, there exists a direct relation between r and *GER*, given in Eq. (4), which can be used to optimize the experimental operating conditions for any M-level quantization scheme. For $M = 2$, *MF* is minimum at $r = 1$, and hence *GER* should be as large as possible. However, for $M = 4$, *MF* is minimum at $r = 0.5$, and substituting it in Eq. (4), we find that the optimal *GER* for best quantization is 9.54 dB. Thus, the *GER* helps to identify the operating point which would correspond to minimum *MF* and hence the best possible phase quantization. It is to be noted that in almost all the literature, GER is mentioned just as a consequence of different mixing ratios. Here, from the very fundamental relation between the GER and mixing ratio, we explore and utilize this measurable quantity as the indirect measure for optimizing the mixing ratio, which is not trivial to optimize otherwise experimentally, especially in SOAs. Thus, even though the GER and mixing ratio is connected through the fundamental relation given in Eq. (4), it is the first time to the best of our knowledge that GER is utilized directly to optimize phase quantization.

Figure 2 shows the normalized power and phase of the quantized output for both two and four level phase quantizations, as a function of input phase (marked in multiples of π). For two-level phase quantization, the mixing ratio $r = 1$, gives the maximum gain extinction ratio (here denoted by the large amplitude dip), as shown in Fig. 2(a), and matches with that obtained from the optimization of the *MF* factor . The corresponding phase quantization output- which is an ideal step function for two level phase quantization - is shown in Fig. 2(b). The figure also shows the output for different values of r, indicating that even a small change in r leads to a large quantization error. Similarly for the four-level quantization, the *MF* is minimized at $r = 0.5$, and

the corresponding phase quantization is found to be the optimal one as shown in Fig. 2(d). Even though the *GER* is found to be larger for values of *r* other than 0.5, the corresponding output phase shows a large quantization error. Thus, in an experiment, it is critical to find the operating condition that gives a *GER* of exactly 9.54 dB, which results in the minimum misfit factor. It is important to note that the optimal *GER* values depend only on *M* and are independent of the nonlinear medium used to achieve phase quantization.
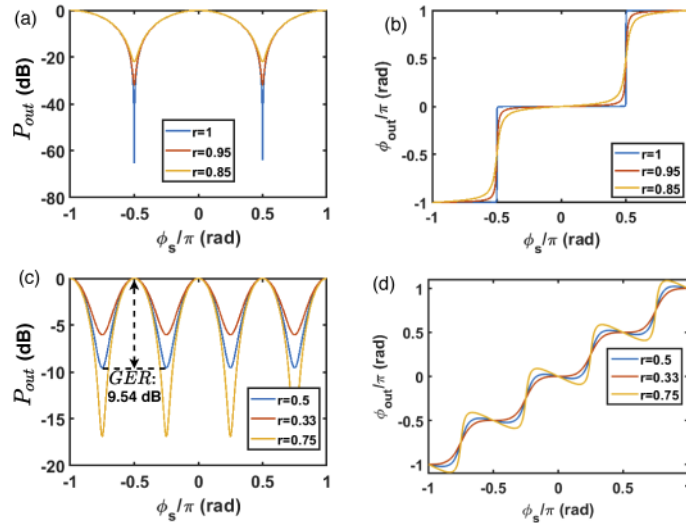

Fig. 2. Quantized output as a function of relative input signal phase (a) Output power (normalized) and (b) Output phase for two-level quantization, (c) Output power (normalized) and (d) Output phase for four-level quantization, for different *r* values.

3. Experimental demonstrations

The basic characterization showing the gain asymmetry of the SOA used in the PSA stage is shown in Fig. 3. The SOAs we used are nonlinear (NL-SOA, Kamelian) with an output saturation power of 10 dBm and gain recovery time of 25 ps. Figure 3 shows both the gain (in black circles) and the conjugate conversion efficiency (in blue squares) as a function of detuning between the signal and the pump frequencies (f_s and f_p respectively) measured experimentally, for the SOA used in the PSA stage, at a drive current of 350 mA. To specifically indicate the gain asymmetry in the presence of pump, the values of gain at a detuning of ± 50 GHz is marked in Fig. 3 (horizontal black dashed lines), and the difference in gain for positive and negative detuning is found to be 6 dB. For the same detuning, the conjugate conversion efficiency (the ratio of the conjugate power to the input signal power) is found to have a difference of 3.5 dB between the positive and negative detuning (indicated as horizontal red dotted lines). It clearly demonstrates the asymmetric behaviour of the SOA in the presence of the pump. Thus, SOA being a gain medium with asymmetry, the optimization explained here in the manuscript is a practically useful technique for obtaining better phase quantization.

3.1. Two-level phase quantization

Two level phase quantization occurs when a signal and its conjugate are allowed to add coherently at the same frequency. The output power and phase response expected of such a coherent addition is shown in Fig. 2(a) and 2(b) respectively.
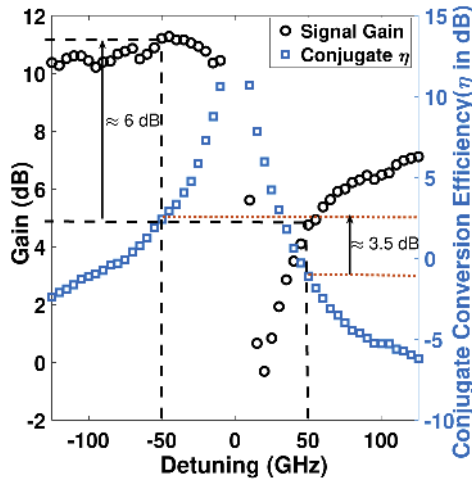
Fig. 3. Gain and conversion efficiency as a function of detuning ($f_s - f_p$).

3.1.1. Implementation

Figure 4 shows a schematic of the experimental setup used to demonstrate two-level phase quantization. The expected spectra at the outputs of different stages are also shown in the figure. This scheme helps to explicitly characterize the phase-to-phase transfer function of a two-level phase quantizer using SOAs and is similar to that demonstrated in [39], where HNLF was used as a nonlinear medium.
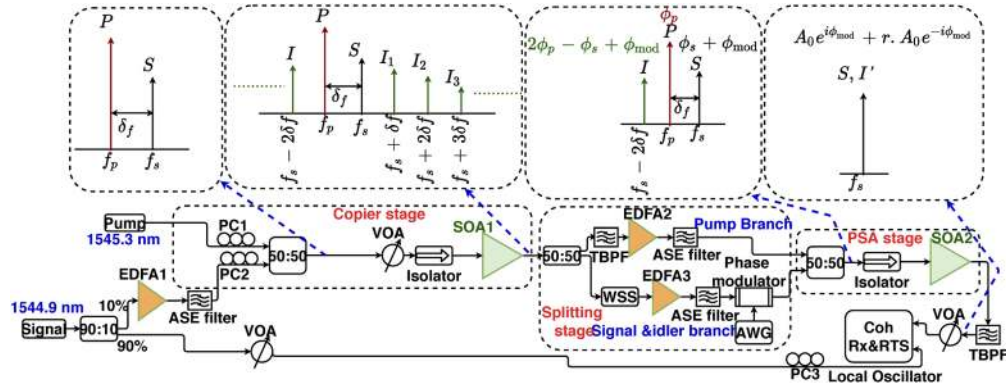

Fig. 4. Experimental setup to study the phase transfer function of PSA for two-level quantization

Two independent narrow-linewidth lasers at frequencies f_p and f_s are used as sources for the pump and signal respectively. The output of the signal laser is split and a part of it is used as the local oscillator for the coherent receiver. The amplified signal is filtered to remove the out-of-band amplified spontaneous emission (ASE) noise, and is combined with the pump using a 3-dB coupler and fed to the first SOA. Using polarisation controllers, it is ensured that the polarisation states of the pump and the signal are matched at the input of the SOA. The first nonlinear mixing stage - referred to as the copier stage - is used to phase-lock the pump, signal and idler of interest through the partially degenerate FWM process in the SOA. A phase conjugate of the signal (I), at frequency $f_I = 2f_p - f_s$ and phase $2\phi_p - \phi_s$ is generated at the output of this

stage. The output of the copier stage is split using a 3-dB coupler. The signal and its conjugate are filtered in one of the arms, and both of them are modulated with a linear phase, $\phi_{mod}(t)$, between $-\pi$ to π rad at 15 MHz using an electro-optic phase modulator. This modulation frequency is chosen such that the output is captured without being influenced by the environmental phase fluctuations. The pump is filtered and amplified in the other arm. The phase-modulated signal (phase $\phi_s + \phi_{mod}(t)$, power S) and its conjugate (phase $2\phi_p - \phi_s + \phi_{mod}(t)$, power I) are combined with the pump (phase ϕ_p, power P) and fed to SOA2 (PSA stage). The idler (I') generated in SOA2 at frequency f_s (= $2f_p - f_I$) and its phase ($\phi_s - \phi_{mod}(t)$) then coherently add with the input signal to yield two level phase quantization. The output of the PSA stage at the signal frequency f_s is filtered and fed to the coherent receiver followed by a real time scope. The I and Q data recorded in the scope is further used to extract the phase of the quantized signal.

3.1.2. Results and discussion

The quality of quantization is determined by the ratio with which the coherent addition of the signal and the desired idler occurs, as discussed in Section 2. Hence, prior to the phase quantization step, we identify this operating condition by measuring the *GER*. In this *GER* optimization step, the output of the copier stage is directly fed to the waveshaper (Finisar-WaveShaper 1000s.) for manually changing the relative phase of the signal and idler at the PSA input. The input and output of the PSA stage are recorded on an optical spectrum analyser (OSA) and the corresponding gain at the signal frequency is measured as a function of input signal phase. The corresponding results are shown in Fig. 5(a).
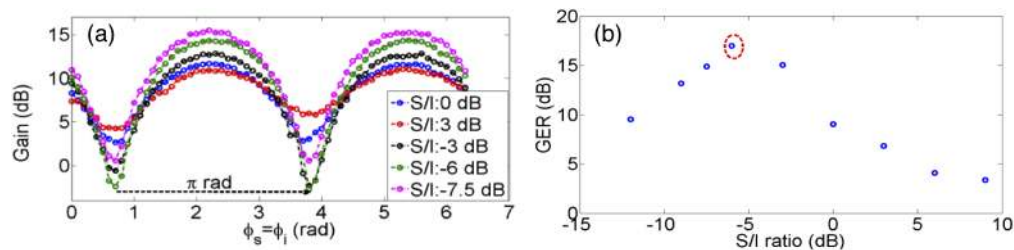

Fig. 5. (a) Gain vs. Relative phase between the signal and pump, (b) *GER* vs. *S/I* ratio (red circle shows the highest *GER* for *S/I* ratio of -6 dB); pump power = 0 dBm

The maximum and minimum gains are observed at a phase difference of $\pi/2$ as expected. We change the pump/signal/idler power ratios at the input of the PSA stage using power attenuation of each filtered line in the waveshaper. For each set of power ratio, we sweep the input relative phase of the signal and idler, using the waveshaper and record the phase sensitive gain (PSG) as a function of input phase. The results are shown in Fig. 5(a). We calculate the *GER* as the ratio of the maximum to the minimum measured gain value. We choose the input pump power such that it is sufficient (0 dBm) to saturate the SOA. We fix the signal to the idler power ratio (*S/I*) and vary the pump/idler (*P/I*) power ratios by changing both the signal and the idler power at the PSA input. *GER* is found to be independent of the *P/I* ratio (not shown here) when it is varied over a range of +14 dB to +26 dB for an *S/I* ratio of 0 dB. We further vary the signal power after fixing the *P/I* ratio to a specific value (+14 dB). This *P/I* ratio was chosen such that, it enables a large range of *S/I* ratio between -15 to +10 dB in the PSA stage. Variation in signal power correspondingly changes the *S/I* ratio while we observe a corresponding large variation in *GER* for each case. The corresponding *GER* as a function of the *S/I* ratio is shown in Fig. 5(b). The largest *GER* is observed for a signal/idler (*S/I*) power ratio of -6 dB.

In order to extract the phase transfer characteristics after the PSA, the optimized values (*S/I* = -6 dB) are further used as the input power levels to the SOA2. Phase modulation using a

saw-tooth waveform at a frequency of 15 MHz is applied in the signal and idler arm, and the applied drive voltage is set such that it swings from $-V_\pi$ to $+V_\pi$ (3.5 V_{pp}) at the input RF port of the modulator. Thus one cycle of saw-tooth RF waveform modulates the input signal and idler phase linearly over 2π radians. Figure 6(a) & (b) shows the input and the output of the phase quantization stage where it is clearly evident that the output is quantized to two fixed phase states with an absolute nonzero mean phase shift (corresponding to the residual ϕ_s).
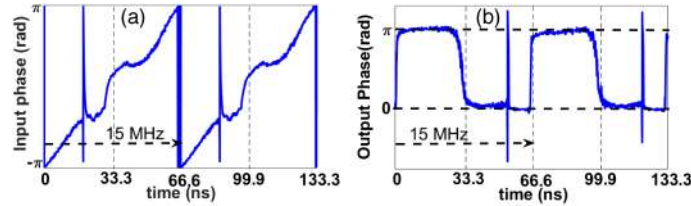

Fig. 6. (a) The phase of the input signal to the phase quantizer obtained by driving a phase modulator with a 15 MHz sawtooth input voltage (b) Two-level phase quantized output of the PSA stage.

The two quantized phase states are found to have a phase difference of π as expected for the two level phase quantizer. The lower quantized values is aligned to 0 rad and the upper quantized one to π for the clear visualization and hence the output phase mentioned here is the relative output phase. Phase jumps in both Fig. 6(a) and (b) are possibly due to phase wrapping between $-\pi$ and $+\pi$ rad, whenever a random phase drifts occurs in the system possibly due to some environmental perturbation, or due to the voltage fluctuations in RF source used to drive the modulator. *GER* is maximum at S/I ratio of -6 dB and near ideal phase quantization is obtained for the optimized power ratio. Other S/I ratios, which resulted in smaller GER in Fig. 5(b) resulted in quantization, albeit with a large quantization error. Note that, this is different from the power ratio for optimized phase quantization in HNLF where the optimal S/I ratio is 0 dB [39]. Even in the case of HNLF, the optimal S/I ratio depends on the specific operating and saturation condition. In this work using SOA, we find that the optimized power ratio (S/I) is not unity. This difference is primarily due to gain asymmetry of the SOA.

These values of different optimized power ratios are all specific to our experiments and can change in different experimental test-beds and experimental conditions, but the optimal GER is independent of the experimental conditions.

3.2. Four-level phase quantization

Four level quantization occurs when the conjugate of the signal coherently adds with its third harmonic, both generated at the same frequency, resulting in a phase addition corresponding to $e^{-i\phi_s} + r.e^{i3\phi_s}$. To obtain the four level phase quantization with the optimized power ratio through the corresponding *GER*, we design a proof of principle experiment, which is modified from that shown for the two-level quantization.

3.2.1. Implementation

The experimental setup used to demonstrate the four-level quantization is shown in Fig. 7. The signal and pump at frequencies f_s and f_p with a detuning $\delta f = f_s - f_p = 50$ *GHz*, are propagated through the copier stage, to result in a cascaded FWM process described below. Idler, I_1 at frequency $2f_s - f_p$ with the phase $2\phi_s - \phi_p$ is generated due to mixing of the pump and signal. This idler mixes with the signal and results in the generation of idler I_2 at frequency $3f_s - 2f_p = f_s + 2\delta f$ with the phase $3\phi_s - 2\phi_p$. I_2 further mixes with I_1 to generate idler I_3, at frequency $4f_s - 3f_p = f_s + 3\delta f$ with the phase $4\phi_s - 3\phi_p$, which would be further used as the

correlated second pump required for the four-level quantization process. Phase quantization occurs at the idler I_2 frequency $f_s + 2\delta f$ in the PSA stage. The output of the copier stage is split and the frequency corresponding to $f_s + 2\delta f$ is filtered in one of the arms, which is further used as a local oscillator for the coherent receiver that is used to measure the phase of the quantized output. The pump and the third harmonic idler I_3 are filtered in the other arm, which is further combined with the phase modulated signal (phase, $\phi_s + \phi_{mod}(t)$) and fed as input to the PSA stage. Note that, unlike in the case of two-level quantization, only the signal is phase modulated using an electro-optic phase modulator driven with a 15 MHz saw tooth wave of V_{pp} so that $\phi_{mod}(t)$ is swept in the range $-\pi$ and $+\pi$ in a linear fashion.
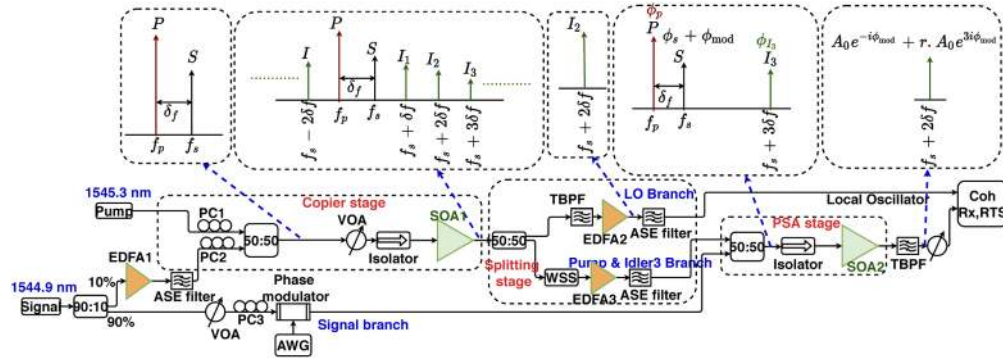

Fig. 7. Experimental setup to demonstrate four-level quantization

In the second SOA, the conjugate I' is generated at frequency $f_p + f_{I3} - f_s = f_s + 2\delta f$, through the mixing of pump, signal and idler I_3, which possesses the conjugate phase of the signal, the time-varying part of which is $-\phi_{mod}(t)$. Similarly, idler I_2 generated in SOA2, through the cascaded mixing process described above, at frequency $f_s + 2\delta f$ with third harmonic phase of the signal ($3\phi_{mod}(t)$). Thus, in the second SOA, the idlers I_2 and I' generated through two independent processes, but at the same frequency, coherently combine and this results in four-level phase quantization.

SOA1 at the copier stage is used here only to generate the phase correlated lines (P and I_3) required for the phase quantization stage. The component, $f_s + 2\delta f$ at the output of SOA1 is unmodulated, and hence if it is fed to the PSA stage (SOA2), it will degrade the coherent addition of the $3f_s - 2f_p$ and $f_p + f_{I3} - f_s$ modulated components, leading to poor quantization. We, however, use the filtered $f_s + 2\delta f$ component from the copier stage (SOA1) as the local oscillator for demonstration of the four-level quantization as shown in Fig. 7. The signal is modulated only at the PSA stage for this proof of principle experiment. If we modulate the signal at the input of the copier stage, the modulated signal with a phase $\phi_s + \phi_{mod}(t)$, would generate idler I_3 at frequency f_{I3} in the copier stage, with a phase $4(\phi_s + \phi_{mod}(t)) - 3\phi_p$. This would result in the signal conjugate I' in the PSA stage to have a phase $\phi_p + (4(\phi_s + \phi_{mod}(t)) - 3\phi_p) - (\phi_s + \phi_{mod}(t)) = 3(\phi_s + \phi_{mod}(t)) - 2\phi_p$, which is identical to the phase of I_2, resulting in phase-sensitive gain with no phase quantization. As discussed in Section 2, the amplitude ratios with which this combination occurs decides the quality of quantization, which is measured and optimized indirectly through *GER*, as discussed below.

3.2.2.   Results and discussion

As in the previous case, we first optimize input power levels into the PSA stage by measuring the *GER*, with CW operation. In the *GER* optimization step, the splitting at the output of copier stage is bypassed, and all the three required waves- signal, pump and the idler I_3, are filtered

using the waveshaper and fed to the second SOA, whose output is monitored using an OSA. The amplitude and phase (from 0 to 2π radians) of the input waves are varied using the waveshaper and the gain as a function of the input signal phase is measured from the spectrum. The optimal ratio with which the pump, signal and idler I_3 has to be fed to the quantization step is determined by monitoring the gain extinction ratio for different values of power ratio of signal to pump (S/P) and pump to idler I_3 (P/I_3). The spectra at the input and output of the PSA stage are shown in Fig. 8(a). The input spectrum (blue) shows the three input waves S, P and I_3. The output spectrum is shown under both the maximum gain (green line) and minimum gain (red line) conditions, where $GER \sim 9.5$ dB is achieved corresponding to the theoretically optimized value at $f_s + 2\delta f$.
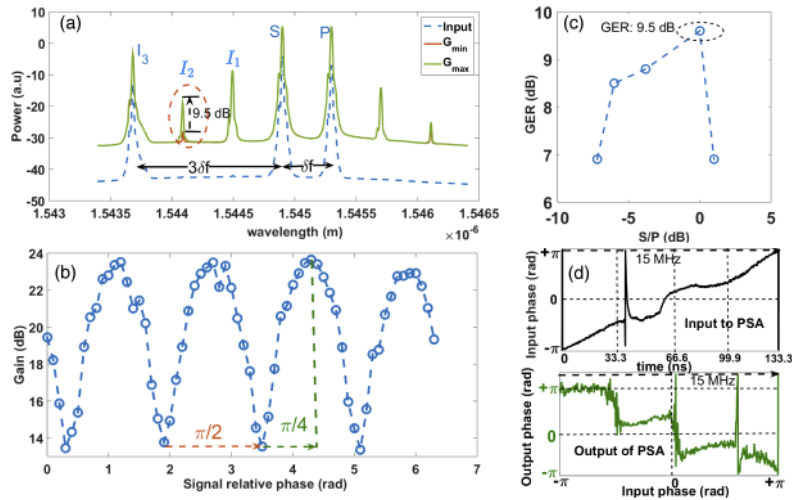

Fig. 8. (a) A reference spectrum at the PSA input, PSA output spectra, corresponding to maximum gain G_{max} and minimum gain G_{min}, of the $f_s + 2\delta f$ component at the PSA based four-level phase quantizer output, (b) Phase-sensitive gain (PSG) vs input relative signal phase (c) Gain extinction ratio (GER) for different S/P ratio for a given P/I_3 ratio, and (d) Input phase at the PSA input (top) and phase transfer function of the four-level phase quantizer (bottom).

The gain at $f_s + 2\delta f$ as a function of signal's relative phase is shown in Fig. 8(b). The maxima and minima are obtained with a phase difference of $\pi/4$ as expected for four-level quantization. Since both the signal and the pump participate in the generation of I' and I_3, the signal to pump power ratio (S/P), which primarily decides the mixing ratio r of I' and I_3 at the PSA stage, is varied and GER is measured for each combination by plotting the phase sensitive gain as a function of input signal phase, for different P/I_3 power ratios and the results are shown in Fig. 8(c). The pump power is fixed to 0 dBm and the pump to I_3 power ratio (P/I_3) is maintained constant at ~6 dB for these experiments. From theoretical predictions the GER of ~9.54 dB would give the best possible four-level quantization. This condition is achieved when the input to the PSA stage is with the ratio P/I_3 of ~6 dB and the S/P of ~0 dB (GER=9.5 dB) as indicated by a black dotted ellipse in Fig. 8(c). Note that, these power ratios would be a function of operating wavelengths. The tolerance range of GER (and the corresponding power ratio) for the optimum quantization is relatively small such that we could not observe four-level phase quantization for other operating conditions.

Now in the phase quantization stage, proper adjustment of the optimized power ratio of interacting waves are precisely carried out by adjusting the amplitude of the corresponding frequencies in the waveshaper, while the signal phase is swept over 2π radians at a faster rate of 15 MHz by driving a phase modulator with a saw-tooth waveform. The output of the SOA2 is

filtered to select the $f_s + 2\delta f$ component. For coherent detection, the local oscillator at $f_s + 2\delta f$ is obtained from the copier stage as shown in Fig. 7. The input and output phase transfer function of the phase quantization step is shown in Fig. 8(d). The imperfection in the quantized output could be attributed to the phase-noise transfer due to the cascaded four wave mixing processes.

   We also observe that the quantized output phase (Fig. 8(d)) has opposite slope when compared to that of the input. This is because the quantization is measured in the conjugate regime, where the coherent addition is between the signal conjugate and third phase harmonics of the signal ($e^{-i\phi_s} + r.e^{i3\phi_s}$). In case the quantization is carried out through the phase addition corresponding to ($e^{i\phi_s} + r.e^{-i3\phi_s}$), this change in slope may be avoided [35]. Since optimization of four-level phase quantization is established, the experiment can now be further extended to illustrate PSA of QPSK modulation formats using SOAs.

4.   Discussion

Phase correlation among the participating waves in the phase quantization process is a necessary condition for quantization to occur with minimal errors. Here this condition is obtained with a copier stage which generates the requisite idlers through cascaded four wave mixing. However, the phase noise of the pump and signal at the input of the copier stage determines the error in phase quantization due to the total phase noise transfer at the quantization frequency. The total phase noise in the case of two-level phase quantization in our experiment is decided by the laser phase noise of the signal. Since we use a laser with a very narrow-linewidth for the signal, the quality of the quantization is not affected significantly. However, the total phase error variance at the quantization frequency for the four-level phase quantization scheme can be calculated as the $3\sigma_s^2 + 2\sigma_p^2$, where σ_s^2 and σ_p^2 refers to the phase error variance of the signal and pump respectively. This is why in our experiments the four-level phase quantization is not ideal. This can be avoided if we use the phase-correlated comb-lines instead of the copier stage. With the comb lines, the expected phase-error variance at the output becomes identical to that of one of the comb lines. Another issue that must be taken care of in the experiment is the handling of the phase fluctuations due to environmental changes. Optical phase-locked loops (OPLL) are typically used to maintain phase correlations in black-box implementations of PSA. In our proof-of-principle experiment, we could avoid the OPLL as we sweep the signal phase much faster than the rate of environmental fluctuation. In actual experiments with BPSK/QPSK data in the signal, the experimental setup should have the OPLL incorporated in order to obtain the phase quantization. Moreover, locally generated pump should be used for a black box-PSA implementation, where the pump is generated through injection locking and carrier recovery [15,17].

5.   Conclusion

We optimize the power ratio of input waves to an SOA-based PSA stage for both two-level and four-level phase quantization schemes. The relation between the mixing ratio r and the measurable quantity *GER* is utilized for power optimization. We experimentally study the effect of *GER* on phase quantization efficiency and obtain the best two-level phase quantization for S/I ratio of -6 dB. Owing to the gain asymmetry of the SOA, the best *GER* and phase quantization are obtained at unequal signal and idler input power levels (S/I= -6 dB). Furthermore the *GER* is optimized for a four-level phase quantization scheme and illustration of the phase-sensitive gain of the four-level phase quantization scheme is experimentally carried out. The *GER* of different S/P ratios is measured and the proper ratio which gives *GER* of ~ 9.5 dB is selected to illustrate four-level phase quantization. Thus for both two-level and four-level phase quantization, *GER* is used as the key parameter for optimization and we successfully achieved the quantization with a pump power requirement of only 0 dBm. The idea could now be extended to demonstrate PSA of BPSK/ QPSK modulation formats using SOAs, with optimised operating conditions.

References

1. P. V. Mamyshev, "All-optical data regeneration based on self-phase modulation effect," vol. 1, pp. 475–476, *ECOC* 1998.
2. T. I. Lakoba and M. Vasilyev, "On multi-channel operation of phase-preserving 2R amplitude regenerator," Opt. Commun. **322**, 114–117 (2014).
3. J. K. Lucek and K. Smith, "All-optical signal regenerator," Opt. Lett. **18**(15), 1226–1228 (1993).
4. J. A. Levenson, I. Abram, T. Rivera, and P. Grangier, "Reduction of quantum noise in optical parametric amplification," J. Opt. Soc. Am. B **10**(11), 2233–2238 (1993).
5. C. M caves, "Quantum limits on noise in linear amplifiers," Phys. Rev. D **26**(8), 1817–1839 (1982).
6. T. Inagaki, K. Inaba, R. Hamerly, K. Inoue, Y. Yamamoto, and H. Takesueet, "Large-scale Ising spin network based on degenerate optical parametric oscillators," Nat. Photonics **10**(6), 415–419 (2016).
7. Z. Y. Ou, "Enhancement of the phase-measurement sensitivity beyond the standard quantum limit by a nonlinear interferometer," Phys. Rev. A **85**(2), 023815 (2012).
8. F. Hudelist, J. Kong, C. Liu, J. Jing, Z. Y. Ou, and W. Zhang, "Quantum metrology with parametric amplifier-based photon correlation interferometers," Nat. Commun. **5**(1), 3049 (2014).
9. P. A. Andrekson and M. Karlsson, "Fiber-based phase-sensitive optical amplifiers and their applications," Adv. Opt. Photonics **12**(2), 367–428 (2020).
10. M. E. Marhic, C. H. Hsia, and J. M. Jeong, "Optical amplification in a nonlinear fibre interferometer," Electron. Lett. **27**(3), 210–211 (1991).
11. A. Takada and W. Imajuku, "Amplitude noise suppression by using high-gain phase-sensitive amplifier as limiting amplifier," paper. WA5, *OFC* 1996.
12. W. Imajuku and A. Takada, "In-line phase-sensitive amplifier with optical-PLL-controlled internal pump light source," Electron. Lett. **33**(25), 2155–2156 (1997).
13. M. Gao, T. Inoue, T. Kurosu, and S. Namiki, "Evolution of the gain extinction ratio in dual-pump phase sensitive amplification," Opt. Lett. **37**(9), 1439–1441 (2012).
14. Z. Zheng, L. An, Z. Li, X. Zhao, and X. Liu, "All-optical regeneration of DQPSK/QPSK signals based on phase-sensitive amplification," Opt. Commun. **281**(10), 2755–2759 (2008).
15. R. Slavík, F. Parmigiani, J. Kakande, C. Lundström, M. Sjödin, P. A. Andrekson, R. Weerasuriya, S. Sygletos, A. D. Ellis, L. G. Nielsen, D. Jakobsen, S. Herstrom, R. Phelan, J. O'Gorman, A. Bogris, D. Syvridis, S. Dasgupta, P. Petropoulos, and D. J. Richardson, "All-optical phase and amplitude regenerator for next-generation telecommunications systems," Nat. Photonics **4**(10), 690–695 (2010).
16. R. Slavik, A. Bogris, J. Kakande, F. Parmigiani, L. Gruner-Nielsen, R. Phelan, J. Vojtech, P. Petropoulos, D. Syvridis, and D. J. Richardson, "Field-Trial of an All-Optical PSK Regenerator/Multicaster in a 40 Gbit/s, 38 Channel DWDM Transmission Experiment," J. Lightwave Technol. **30**(4), 512–520 (2012).
17. J. Kakande, R. Slavík, F. Parmigiani, A. Bogris, D. Syvridis, L. G. Nielsen, R. Phelan, P. Petropoulos, and D. J. Richardson, "Multilevel quantization of optical phase in a novel coherent parametric mixer architecture," Nat. Photonics **5**(12), 748–752 (2011).
18. J. Kakande, R. Slavík, F. Parmigiani, P. Petropoulos, and D. J. Richardson, "All-Optical Processing of Multi-level Phase Shift Keyed Signals," paper OW1I.3, *OFC* 2012.
19. R. Slavík, A. Bogris, F. Parmigiani, J. Kakande, M. Westlund, M. Sköld, L. Grüner-Nielsen, R. Phelan, D. Syvridis, P. Petropoulos, and D. J. Richardson, "Coherent All-Optical Phase and Amplitude Regenerator of Binary Phase-Encoded Signals," IEEE J. Sel. Top. Quantum Electron. **18**(2), 859–869 (2012).
20. F. Parmigiani, K. R. H. Bottrill, R. Slavík, D. J. Richardson, and P. Petropoulos, "Multi-Channel phase regenerator based on polarization-assisted phase-sensitive amplification," IEEE Photonics Technol. Lett. **28**(8), 845–848 (2016).
21. H. Wang, C. He, G. Li, and Y. Ji, "All-Optical Phase Quantization with High Accuracy Based on a Multiwave Interference Phase Sensitive Amplifier," IEEE Photonics J. **9**(3), 1–8 (2017).
22. M. E. Marhic, "Polarization independence and phase-sensitive parametric amplification," J. Opt. Soc. Am. B **28**(11), 2685–2689 (2011).
23. J. Yang, M. Ziyadi, Y. Akasaka, S. Khaleghi, M. R. Chitgarha, J. Touch, and M. Sekiya, "Investigation of polarization-insensitive phase regeneration using polarization-diversity phase-sensitive amplifier," pp. 1–3, *ECOC* 2013.
24. A. L. Riesgo, C. Lundström, F. Chiarello, M. Karlsson, and P. A. Andrekson, "Phase-sensitive amplification and regeneration of dual-polarization BPSK without polarization diversity," pp. 1–3, *ECOC* 2014.
25. W. Yang, Y. Yu, M. Ye, G. Chen, C. Zhang, and X. Zhang, "Phase regeneration for polarization-division multiplexed signals based on vector dual-pump nondegenerate phase sensitive amplification," Opt. Express **23**(3), 2010–2020 (2015).

26. A. Lorences-Riesgo, P. A. Andrekson, and M. Karlsson, "Polarization-Independent Phase-Sensitive Amplification," J. Lightwave Technol. **34**(13), 3171–3180 (2016).

27. B. J. Puttnam, D. Mazroa, S. Shinada, and N. Wada, "Phase-squeezing properties of non-degenerate PSAs using PPLN waveguides," Opt. Express **19**(26), B131–B139 (2011).

28. T. Umeki, M. Asobe, and H. Takenouchi, "In-line phase sensitive amplifier based on PPLN waveguides," Opt. Express **21**(10), 12077–12084 (2013).

29. T. Umeki, T. Kazama, O. Tadanaga, K. Enbutsu, M. Asobe, Y. Miyamoto, and H. Takenouchi, "PDM Signal Amplification Using PPLN-Based Polarization-Independent Phase-Sensitive Amplifier," J. Lightwave Technol. **33**(7), 1326–1332 (2015).

30. M. A. Ettabib, K. Bottrill, F. Parmigiani, A. Kapsalis, A. Bogris, M. Brun, P. Labeye, S. Nicoletti, K. Hammani, D. Syvridis, D. J. Richardson, and P. Petropoulos, "PSA-based phase regeneration of DPSK signals in a silicon germanium waveguide," pp. 1–3, *ECOC* 2015.

31. M. A. Ettabib, K. Bottrill, F. Parmigiani, A. Kapsalis, A. Bogris, M. Brun, P. Labeye, S. Nicoletti, K. Hammani, D. Syvridis, D. J. Richardson, and P. Petropoulos, "All-optical phase regeneration with record PSA extinction ratio in a low-birefringence silicon germanium waveguide," J. Lightwave Technol. **34**(17), 3993–3998 (2016).

32. F. Da Ros, M. Pu, L. Ottaviano, H. Hu, E. Semenova, M. Galili, K. Yvind, and L. K. Oxenlowe, "Phase-sensitive four-wave mixing in AlGaAs-on-insulator nano-waveguides," pp. 505–506, *IPC* 2016.

33. W. Li, M. Lu, A. Mecozzi, M. Vasilyev, S. Arafin, D. Dadic, L. A. Johansson, and L. A. Coldren, "First Monolithically Integrated Dual-Pumped Phase-Sensitive Amplifier Chip Based on a Saturated Semiconductor Optical Amplifier," IEEE J. Quantum Electron. **52**(1), 1–12 (2016).

34. A. D. Ellis and S. Sygletos, "Phase Sensitive Signal Processing using Semiconductor Optical Amplifiers," paper OW4C.1, *OFC* 2013.

35. K. R. H. Bottrill, R. Kakarla, F. Parmigiani, D. Venkitesh, and P. Petropoulos, "Phase Regeneration of QPSK Signal in SOA Using Single-Stage, Wavelength Converting PSA," IEEE Photonics Technol. Lett. **28**(2), 205–208 (2016).

36. A. Sobhanan, V. A. M. Karthik, L. V. Narayanan, R. D. Koilpillai, and D. Venkitesh, "Experimental Analysis of Noise Transfer in Optical Phase Conjugation Process in Nonlinear SOA," paper W2A.38, *OFC* 2019.

37. A. Sobhanan and D. Venkitesh, "Low-distortion amplification of single channel QPSK/16QAM signals using SOA with HBeam," paper. SpM2I.5, *SPPCom* 2020.

38. C. Lundström, B. Corcoran, M. Karlsson, and P. A. Andrekson, "Phase and amplitude characteristics of a phase-sensitive amplifier operating in gain saturation," Opt. Express **20**(19), 21400–21412 (2012).

39. C. Lundström, Z. Tong, M. Karlsson, and P. A. Andrekson, "Phase-to-phase and phase-to-amplitude transfer characteristics of a nondegenerate-idler phase-sensitive amplifier," Opt. Lett. **36**(22), 4356–4358 (2011).

40. J. Kakande, C. Lundström, P. A. Andrekson, Z. Tong, M. Karlsson, P. Petropoulos, F. Parmigiani, and D. J. Richardson, "Detailed characterization of a fiber-optic parametric amplifier in phase-sensitive and phase-insensitive operation," Opt. Express **18**(5), 4130–4137 (2010).

41. Z. Tong, C. Lundström, M. Karlsson, M. Vasilyev, and P. A. Andrekson, "Noise performance of a frequency nondegenerate phase-sensitive amplifier with unequalized inputs," Opt. Lett. **36**(5), 722–724 (2011).

42. H. Wang, T. Liu, K. Tong, Y. Ji, and L. Bai, "Analytical Solution of Amplitude Ratio in Optical Phase Quantization Based on Phase Sensitive Amplification," J. Lightwave Technol. **36**(16), 3396–3402 (2018).

43. A. Iyer, A. Sobhanan, and D. Venkitesh, "Optimization of Four- Wave Mixing Based Multilevel Phase Quantization Through Gain Extinction Ratio," pp. 1–3, *IEEE Workshop on Recent Advances in Photonics*, 2017.

44. F. Parmigiani, G. D. Hesketh, R. Slavík, P. Horak, P. Petropoulos, and D. J. Richardson, "Optical Phase Quantizer Based on Phase Sensitive Four Wave Mixing at Low Nonlinear Phase Shifts," IEEE Photonics Technol. Lett. **26**(21), 2146–2149 (2014).

45. A. Almaiman, Y. Cao, A. M. Ariaei, M. Ziyadi, P. Liao, C. Bao, F. Alishahi, A. Fallahpour, B. Shamee, Y. Akasaka, T. Ikeuchi, S. Wilkinson, J. D. Touch, M. Tur, and A. E. Willner, "Phase-sensitive QPSK channel phase quantization by amplifying the fourth-harmonic idler using counter-propagating Brillouin amplification," Opt. Commun. **423**, 48–52 (2018).

46. S. Sygletos, M. J. Power, F. C. Garcia Gunning, R. P. Webb, R. J. Manning, and A. D. Ellis, "Simultaneous dual channel phase regeneration in SOAs," pp. 1–3, *ECOC* 2012.

47. H. Sun, K. Y Wang, and A. C. Foster, "Pump-degenerate phase-sensitive amplification in amorphous silicon waveguides," Opt. Lett. **42**(18), 3590–3593 (2017).

48. Y. Zhang, C. Husko, J. Schröder, S. Lefrancois, I. H. Rey, T. F. Krauss, and B. J. Eggleton, "Phase-sensitive amplification in silicon photonic crystal waveguides," Opt. Lett. **39**(2), 363–366 (2014).

49. K. J. Lee, F. Parmigiani, S. Liu, J. Kakande, P. Petropoulos, K. Gallo, and D. Richardson, "Phase sensitive amplification based on quadratic cascading in a periodically poled lithium niobate waveguide," Opt. Express **17**(22), 20393–20400 (2009).

50. S. Liu, K. Jo Lee, F. Parmigiani, J. Kakande, K. Gallo, P. Petropoulos, and D. J. Richardson, "Phase-regenerative wavelength conversion in periodically poled lithium niobate waveguides," Opt. Express **19**(12), 11705–11715 (2011).

51. S. L. I. Olsson, M. Karlsson, and P. A. Andrekson, "Nonlinear phase noise mitigation in phase-sensitive amplified transmission systems," Opt. Express **23**(9), 11724–11740 (2015).